

## Strong Suppression of the Spin Hall Effect in the Spin Glass State

Y. Niimi,<sup>1,\*</sup> M. Kimata,<sup>1</sup> Y. Omori,<sup>1</sup> B. Gu,<sup>2</sup> T. Ziman,<sup>3,4</sup> S. Maekawa,<sup>2,5</sup> A. Fert,<sup>6</sup> and Y. Otani<sup>1,7</sup>

<sup>1</sup>*Institute for Solid State Physics, University of Tokyo, 5-1-5 Kashiwa-no-ha, Kashiwa, Chiba 277-8581, Japan*

<sup>2</sup>*Advanced Science Research Center, Japan Atomic Energy Agency, Tokai 319-1195, Japan*

<sup>3</sup>*Institut Laue Langevin, Boîte Postale 156, F-38042 Grenoble Cedex 9, France*

<sup>4</sup>*LPMMC (UMR 5493), Université Grenoble Alpes and CNRS, 25 rue des Martyrs, B.P. 166, 38042 Grenoble, France*

<sup>5</sup>*ERATO, Japan Science and Technology Agency, Sendai 980-8577, Japan*

<sup>6</sup>*Unité Mixte de Physique CNRS/Thales, 91767 Palaiseau France associée à l'Université de Paris-Sud, 91405 Orsay, France*

<sup>7</sup>*RIKEN-CEMS, 2-1 Hirosawa, Wako, Saitama 351-0198, Japan*

(Received 30 June 2015; revised manuscript received 29 September 2015; published 6 November 2015)

We have measured spin Hall effects in spin glass metals, CuMnBi alloys, with the spin absorption method in the lateral spin valve structure. Far above the spin glass temperature  $T_g$  where the magnetic moments of Mn impurities are randomly frozen, the spin Hall angle of a CuMnBi ternary alloy is as large as that of a CuBi binary alloy. Surprisingly, however, it starts to decrease at about  $4T_g$  and becomes as little as 7 times smaller at  $0.5T_g$ . A similar tendency was also observed in anomalous Hall effects in the ternary alloys. We propose an explanation in terms of a simple model considering the relative dynamics between the localized moment and the conduction electron spin.

DOI: [10.1103/PhysRevLett.115.196602](https://doi.org/10.1103/PhysRevLett.115.196602)

PACS numbers: 72.25.Ba, 75.50.Lk, 75.70.Cn, 75.75.-c

Spin glass is one of the magnetic ordering phases with very complex structures, and has been studied for several decades [1]. It typically appears when magnetic impurities are randomly distributed in a nonmagnetic host metal. Below a certain temperature, the so-called spin glass temperature  $T_g$ , magnetic moments at the impurity sites start to order, but since their spatial distribution is random, the Ruderman-Kittel-Kasuya-Yosida interactions between the spins mediated by conduction electrons are also random. Consequently, the ground state of the spin glass is not a simple phase such as a ferromagnet or antiferromagnet but these two are intricately distributed and the randomness induces a large frustration between the spins. Since the spin glass can be regarded as a model system of information science and also the brain [2], it is important to understand the spin glass system more deeply.

Among several spin glass materials, Mn-doped Cu (CuMn) is one of the typical spin glass systems and has been studied mainly by magnetization measurements [3–5]. The magnetic susceptibility shows a typical cusp at  $T_g$  under zero field cooling (ZFC), and it is constant under field cooling (FC). However, some fundamental questions still remain unsolved. While the magnetization is very sensitive to the applied magnetic field, the transport properties are quite robust for the field [6,7], which is different from another typical spin glass metal, AuFe, where the magnetization is proportional to the Hall resistivity [8–10]. Moreover, not only the complex ground state in the spin glass but also spin fluctuations related to the spin chirality [11] have not been fully understood yet. To reveal such properties in the spin glass systems, another type of measurement is highly desirable.

In this Letter, we present spin transport measurements in CuMn. Among several types of spin transport measurements, here we chose spin Hall effect (SHE) measurements using the spin absorption method in the lateral spin valve structure. This method enables us to estimate quantitatively the spin Hall (SH) angle, conversion yield between charge and spin currents, and the spin diffusion length on the same device [12–14]. As a matter of fact, CuMn does not show a clear SHE signal because Mn is not a good scatterer for the spin current [15,20]. Thus, we added a heavy metal impurity in CuMn [20–23]. In the present Letter, we measured the SHE in CuMnBi ternary alloy. We have already shown that Bi in Cu works as a very good skew scatterer and the SH angle of CuBi is very large [13]. When a pure spin current, flow of only the spin angular momentum, is injected into the ternary alloy, it is converted into a charge current at the Bi impurity site through the inverse process of SHE. The converted charge current also feels spin fluctuations at the Mn sites [see Fig. 1(a)]. Surprisingly, the SH angle of CuMnBi starts to decrease at about  $4T_g$  and becomes 7 times smaller compared to that of CuBi at  $0.5T_g$ . This reduction stems from randomized directions of conduction electron spins due to the fluctuating Mn moments.

We prepared two types of devices to evaluate the SHE in the spin glass system. One is for the SHE measurement using the lateral spin valve and the other is for the anomalous Hall effect (AHE) measurement with a simple Hall bar structure. The latter measurement was originally performed by Fert *et al.* using CuMnX (X, transition metal) ternary alloys [20]. In their case, a small amount of Mn was added in Cu. Thus, the interaction between the Mn impurities could be ignored, and the localized moments at

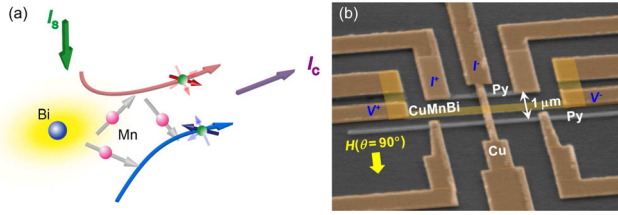


FIG. 1 (color online). (a) Illustration of ISHE in CuMnBi ternary alloy. A pure spin current  $I_s$  is converted into a charge current  $I_c$  at the Bi site. Red and blue arrows with green spheres are spins of conduction electrons ( $|e|$ ) and the shadows indicate that the conduction electron spins are randomized by the localized moments at the Mn sites. The curved arrows show the motions of spin-up and spin-down electrons. (b) Scanning electron micrograph of a typical device. The current leads and voltage probes are for the ISHE measurement.

the Mn sites simply followed a Curie law and worked as spin polarizers. In the present case, the concentration of Mn is much higher than in Ref. [20]. As we will see later on, the Mn impurities work as spin polarizers above a certain temperature ( $T^*$ ), while they interact with each other below this temperature.

Figure 1(b) shows a scanning electron microscopy image of a typical SHE device. It consists of two ferromagnetic permalloy ( $\text{Ni}_{81}\text{Fe}_{19}$ , hereafter Py) wires and a CuMnBi middle wire. These three wires are bridged by a non-magnetic Cu wire. Further details on the SHE device should be referred to in the Supplemental Material [15]. In this Letter, we have fixed the concentration of Bi at 0.5%, which shows the largest SHE signal among CuBi binary

alloys [13], and changed the concentration of Mn from 0% to 1.5%. To check the reproducibility, six different devices have been measured for each Mn concentration.

We first measured the inverse SHE (ISHE) and direct SHE (DSHE) in CuMnBi. When the electric current  $I$  flows from the upper Py wire to the upper side of the Cu wire [see Fig. 1(b)], the resulting spin accumulation at the interface between the Py and Cu wires induces a pure spin current (exactly the same but opposite flows of spin-up and spin-down electrons) only on the lower side of the Cu wire. Most of the generated pure spin current is then absorbed vertically into the CuMnBi middle wire below Cu because of its stronger spin-orbit interaction. Both spin-up and spin-down electrons are deflected to the same direction by the ISHE, and a voltage is generated to prevent a charge current along the wire direction. By inverting the probe configuration (i.e.,  $I^+ \leftrightarrow V^+$ ,  $I^- \leftrightarrow V^-$ ), we can also measure the DSHE; with an electric current in the CuMnBi wire, the spin accumulation induced at the interface between Cu and CuMnBi can be detected as the nonlocal voltage between Py and Cu. For the DSHE measurement, the positive field is defined as the opposite direction to that in Fig. 1(b).

In Figs. 2(a)–2(c), we show the ISHE and DSHE resistances ( $R_{\text{SHE}} \equiv V/I$ ) of  $\text{Cu}_{98}\text{Mn}_{1.5}\text{Bi}_{0.5}$  measured at  $T = 10, 20,$  and  $30$  K.  $R_{\text{SHE}}$  linearly changes with increasing the magnetic field  $H$  and is saturated above  $2000$  Oe, which is the saturation field of the magnetization of the Py wire [12–14]. At any temperature, both the ISHE and DSHE resistances have the same amplitude  $\Delta R_{\text{SHE}}$ , which demonstrates the Onsager reciprocal relation in this

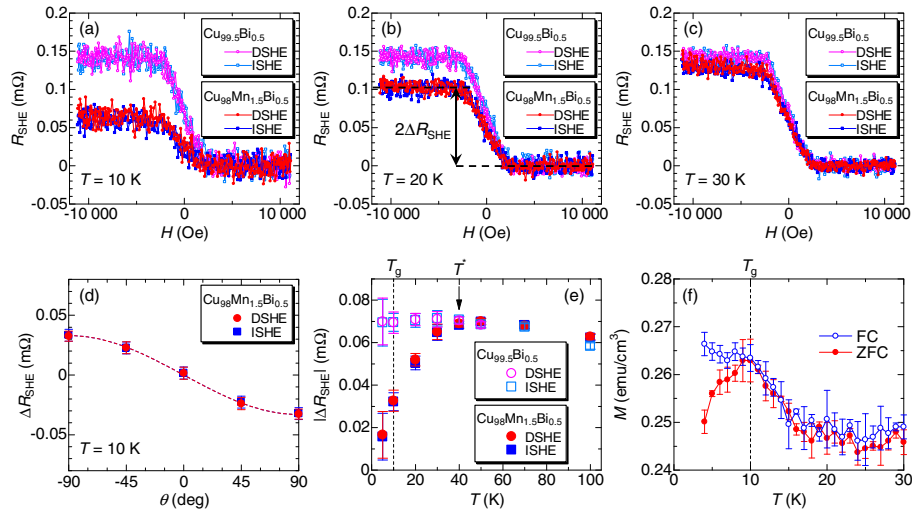


FIG. 2 (color online). (a)–(c) ISHE (closed square) and DSHE (closed circle) resistances ( $R_{\text{SHE}}$ ) of  $\text{Cu}_{98}\text{Mn}_{1.5}\text{Bi}_{0.5}$  measured at  $T = 10, 20,$  and  $30$  K. For comparison,  $R_{\text{SHE}}$  of  $\text{Cu}_{99.5}\text{Bi}_{0.5}$  (open square and circle) are also plotted in the same figures. The amplitude of the SHE resistance  $\Delta R_{\text{SHE}}$  is defined in (b). Both  $R_{\text{SHE}}$  of  $\text{Cu}_{98}\text{Mn}_{1.5}\text{Bi}_{0.5}$  and  $\text{Cu}_{99.5}\text{Bi}_{0.5}$  are shifted along the vertical direction to see the difference of their amplitudes clearly. (d) Magnetic field angle ( $\theta$ ) dependence of  $\Delta R_{\text{SHE}}$  of  $\text{Cu}_{98}\text{Mn}_{1.5}\text{Bi}_{0.5}$  at  $T = 10$  K. The broken curve shows  $-\Delta R_{\text{SHE}}(\theta = 90^\circ) \sin \theta$ . (e)  $|\Delta R_{\text{SHE}}|$  of  $\text{Cu}_{98}\text{Mn}_{1.5}\text{Bi}_{0.5}$  (closed symbols) and  $\text{Cu}_{99.5}\text{Bi}_{0.5}$  (open symbols) as a function of  $T$ . The vertical broken line indicates the spin glass temperature  $T_g$  of  $\text{Cu}_{98}\text{Mn}_{1.5}\text{Bi}_{0.5}$ . The arrow shows the temperature ( $T^*$ ) at which  $|\Delta R_{\text{SHE}}|$  starts to decrease. (f) Magnetizations of  $\text{Cu}_{98}\text{Mn}_{1.5}\text{Bi}_{0.5}$  measured under ZFC (closed symbol) and FC (open symbol) at a small magnetic field ( $H = 50$  Oe) as a function of  $T$ . From the cusp position (the vertical broken line),  $T_g$  can be determined.

system. We have also checked the field angle dependence of  $\Delta R_{\text{SHE}}$  in Fig. 2(d), and found that it follows a sinusoidal curve, typical of SHEs in nonmagnetic metals [14]. Most remarkable is the temperature dependence of  $|\Delta R_{\text{SHE}}|$ .  $|\Delta R_{\text{SHE}}|$  of  $\text{Cu}_{98}\text{Mn}_{1.5}\text{Bi}_{0.5}$  increases with increasing  $T$ , while that of  $\text{Cu}_{99.5}\text{Bi}_{0.5}$  is basically constant up to 30 K. As summarized in Fig. 2(e), the former reaches the latter at 50 K, and both have the same amplitude above 50 K. This fact clearly shows that the large reduction in  $|\Delta R_{\text{SHE}}|$  of  $\text{Cu}_{98}\text{Mn}_{1.5}\text{Bi}_{0.5}$  below  $T^* = 40$  K originates from the additional Mn impurities.

We next changed the Mn concentration down to 0%. Figure 3(a) shows SHE resistivities  $|\rho_{\text{SHE}}^{\text{3D}}|$  of CuMnBi ternary alloys, obtained with a three-dimensional (3D) spin diffusion model [13,14], divided by the resistivity induced by the Bi impurities  $\rho_{\text{Bi}}$ . As demonstrated in our previous works [12–14], in Cu-based alloys,  $\rho_{\text{SHE}}^{\text{3D}}/\rho_{\text{Bi}}$  corresponds to the SH angle  $\alpha_H^{\text{3D}}$ . Basically,  $|\alpha_H^{\text{3D}}|$  has the same tendency as  $|\Delta R_{\text{SHE}}|$ :  $|\alpha_H^{\text{3D}}|$  of  $\text{Cu}_{98}\text{Mn}_{1.5}\text{Bi}_{0.5}$  starts to decrease at  $T^* = 40$  K, while  $|\alpha_H^{\text{3D}}|$  of  $\text{Cu}_{99.5}\text{Bi}_{0.5}$  is constant. Interestingly,  $|\alpha_H^{\text{3D}}|$  of  $\text{Cu}_{98}\text{Mn}_{1.5}\text{Bi}_{0.5}$  at 5 K is reduced by a factor of 7, compared to that at 50 K and also  $|\alpha_H^{\text{3D}}|$  of  $\text{Cu}_{99.5}\text{Bi}_{0.5}$  at 5 K. With decreasing the Mn concentration from 1.5 to 0%,  $T^*$  is shifted to the lower temperature side, and thus the total reduction of  $|\alpha_H^{\text{3D}}|$  at 5 K gets smaller.

In order to relate the reduction of  $|\alpha_H^{\text{3D}}|$  with spin glass, we measured magnetizations  $M$  of  $\text{Cu}_{98}\text{Mn}_{1.5}\text{Bi}_{0.5}$  films under ZFC and FC in Fig. 2(f). A clear cusp was observed at  $T = 10$  K in the ZFC measurement, while the magnetization was saturated for FC. From the cusp position, we can determine  $T_g$  of  $\text{Cu}_{98}\text{Mn}_{1.5}\text{Bi}_{0.5}$  to be 10 K, which is consistent with that of CuMn binary alloys [3]. By combining the SHE and magnetization measurements of CuMnBi, we argue that the reduction of  $|\alpha_H^{\text{3D}}|$  already starts at 4 times higher temperature than  $T_g$  (i.e.,  $T^* = 4T_g$ ) and still continues at  $0.5T_g$ .

What is the origin of the large reduction of  $|\alpha_H^{\text{3D}}|$  below  $T^*$ ? One possibility is related to the spin diffusion of

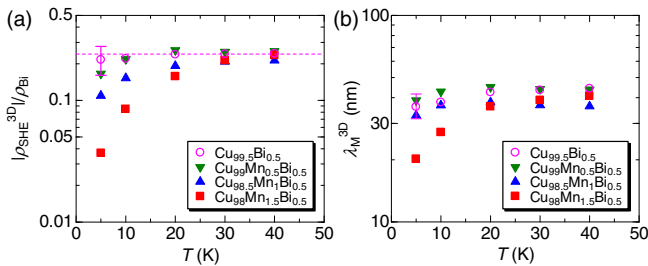


FIG. 3 (color online). (a) SHE resistivities of CuMnBi  $|\rho_{\text{SHE}}^{\text{3D}}|$ , obtained with the 3D calculation, divided by the resistivity induced by the Bi impurities  $\rho_{\text{Bi}}$  as a function of  $T$ . The Bi concentration is fixed at 0.5%, while the Mn concentration is changed from 0 to 1.5%. The broken line in the figure shows  $|\alpha_H^{\text{3D}}|$  of  $\text{Cu}_{99.5}\text{Bi}_{0.5}$ . (b) Spin diffusion lengths of CuMnBi  $\lambda_M^{\text{3D}}$  obtained with the 3D calculation as a function of  $T$ .

conduction electrons in the spin glass state, as observed in electron spin resonance measurements with AgMn and CuMn [24–27] where the spin relaxation of Mn moments is detected. However, this possibility can be ruled out for the following reasons: Based on the simple spin transport model in the skew scattering regime [28],  $\alpha_H \propto 1/(\rho_M \lambda_M)$  but  $\lambda_M \propto 1/\rho_M$  where  $\rho_M$  and  $\lambda_M$  are the resistivity and the spin diffusion length of CuMnBi, respectively. Thus,  $\alpha_H$  is independent of those parameters. As can be seen in Fig. 3(b), the spin diffusion length  $\lambda_M^{\text{3D}}$  estimated from nonlocal spin valve measurements [14] decreases by a factor of 2 for  $\text{Cu}_{98}\text{Mn}_{1.5}\text{Bi}_{0.5}$  as  $T$  approaches  $T_g$ , and shows much less temperature dependence for other Mn concentrations. On the other hand,  $\rho_M$  shows a very small reduction (less than 1%) below  $T^*$  (see Fig. S3 in Ref. [15]). These temperature dependencies of  $\lambda_M$  and  $\rho_M$  completely fail to explain the large suppression of  $\alpha_H$  of CuMnBi below  $T^*$ .

The mechanism we then propose is that the relative dynamics of the polarization of the electron spin  $\vec{s}$  and the localized moments leads to a random precession of  $\vec{s}$ . This reduces the converted charge current  $\vec{I}_C (\propto \vec{I}_S \times \vec{s})$  strongly because of the vector product. At high temperatures, the Mn moments fluctuate quickly and for the spin current the precession is negligible. As the spin glass freezes, the dynamics slows and correlations of the Mn moments decay with a characteristic frequency  $\nu(T)$  which vanishes as a power law as we approach  $T_g$  from above, just as has been seen in experiments with neutrons and muons on bulk spin glasses [29]. This can be understood as the effect of motional narrowing.

We now use a simple phenomenological model, as previously used to model the broadening of the conduction electron spin resonance in metallic spin glasses close to freezing [30]. The polarization  $\vec{s}$  precesses in an effective time-varying magnetic field  $\vec{S}_{\text{eff}}(t)$ , as well as a constant  $\vec{S}_0$  that includes any applied external field:  $(\partial \vec{s} / \partial t) = \vec{s} \times (\vec{S}_0 + \vec{S}_{\text{eff}}(t))$ . The instantaneous  $\vec{S}_{\text{eff}}(t)$  is random in both direction and magnitude, with a distribution width proportional to the  $s$ - $d$  interaction, and fluctuates on a time scale of  $\nu^{-1}(T)$ . For an appropriate choice of  $\vec{S}_{\text{eff}}(t)$ , the integration of the time-dependent equation for  $\vec{s}$  defines the Kubo-Toyabe model [31] as used in muon experiments. For all frequencies, the skew scattered current is reduced from the temperature independent  $\alpha_H$  to  $\alpha_H \langle s \rangle$  where  $\langle s \rangle = G_z [t = \tau_{\text{sk}}, \nu = \nu(T)]$ .  $G_z$  is the average spin correlation with respect to its initial polarization. During the skew scattering, that takes place in a time  $t = \tau_{\text{sk}}$  [32], and the polarization precesses in  $\vec{S}_{\text{eff}}$  that varies with the frequency  $\nu(T)$ . Well above  $T_g$ , we are in the motionally narrowed limit of large  $\nu(T)$  where  $G_z$  is 1. For lower temperatures,  $G_z$  decreases with  $\nu(T)$  and  $\alpha_H$  is reduced (see Fig. S8 in Ref. [15]).



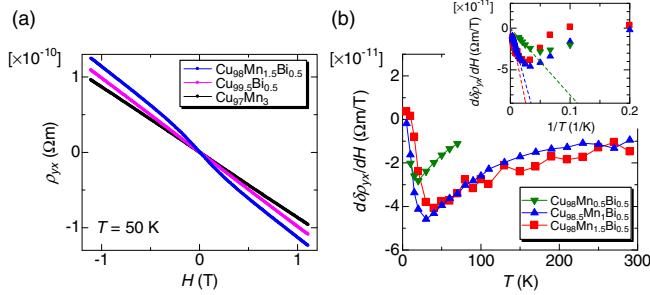


FIG. 4 (color online). (a) Hall resistivities  $\rho_{yx}$  of  $\text{Cu}_{98}\text{Mn}_{1.5}\text{Bi}_{0.5}$ ,  $\text{Cu}_{99.5}\text{Bi}_{0.5}$ , and  $\text{Cu}_{97}\text{Mn}_3$  measured with Hall bars at  $T = 50$  K. (b) Differential values of anomalous parts  $d\delta\rho_{yx}/dH$  for CuMnBi as a function of  $T$ . In the inset, they are plotted as a function of  $1/T$ . The broken lines show the linear fits to obtain  $\alpha_H$ .

As shown above, the SHE in spin glass depends strongly on  $T$ . However, it is quite robust for the applied magnetic field. In the SHE measurements, there is no difference between ZFC and FC even under  $H = 1$  T. This fact looks inconsistent with magnetization measurements [3] but is consistent with the previous transport measurements [6,7]. In addition, recent SHE measurements [33,34] reveal that *homogenous* magnetizations such as ferromagnetic and antiferromagnetic states are irrelevant for the amplitudes of SHE signals. This indicates that the *spin fluctuations* severely affect  $\alpha_H(T)$  and the energy scale of the fluctuations is significantly larger than the applied field. The spin diffusion length, on the other hand, is also affected by the fluctuating fields, but is less sensitive to them than  $\alpha_H(T)$  [see Fig. 3(b)].

To support our findings in the SHEs in CuMnBi, we have also performed the AHE measurements. When the Mn concentration is low enough, Mn works as a spin polarizer and its magnetization follows a simple Curie law, i.e.,  $M \propto T^{-1}$ . On the other hand, Mn does not work as a skew scatterer [15,20]. Thus, to see the spin-dependent transport in Cu-based alloys, an additional metal with stronger spin-orbit interaction is needed, as detailed in Ref. [20]. Figure 4(a) shows a typical Hall resistivity of  $\text{Cu}_{98}\text{Mn}_{1.5}\text{Bi}_{0.5}$  at  $T = 50$  K. As reference signals, we also plot the Hall resistivities  $\rho_{yx}$  of  $\text{Cu}_{99.5}\text{Bi}_{0.5}$  and  $\text{Cu}_{97}\text{Mn}_3$  at the same temperature. Only for  $\text{Cu}_{98}\text{Mn}_{1.5}\text{Bi}_{0.5}$ , an anomaly can be seen near 0 T.

The anomalous part  $d\delta\rho_{yx}/dH$  can be extracted by subtracting the derivation of  $\rho_{yx}$  at zero field from the one of normal Hall resistivity at 1 T. As demonstrated in Ref. [20], by plotting  $d\delta\rho_{yx}/dH$  as a function of  $1/T$ ,  $\alpha_H$  of CuBi can be evaluated [see the inset of Fig. 4(b) and Ref. [15]]. It is  $-0.23(\pm 0.06)$ , which is quantitatively consistent with  $\alpha_H^{\text{3D}}$  determined by the SHE device [13]. As we decrease  $T$ , the amplitude of  $|d\delta\rho_{yx}/dH|$  increases inversely proportional to  $T$ , but it starts to decrease at the exactly same temperature as  $T^*$  [see Fig. 4(b)]. A similar

tendency can also be seen in CuMnIr ternary alloys (see Ref. [15] for more details).

Finally, let us discuss the difference between the two typical spin glass materials, CuMn and AuFe. As mentioned in the introduction, in AuFe, both the magnetization and the AHE show the same temperature and field dependencies [10], while such behavior cannot be seen in CuMn. This can be explained as follows. Mn has a magnetic moment but it does not function as a skew scatterer for conduction electron spins. Thus, an additional skew-scatterer “X” is added and the interaction of the Mn moments on spin currents occurs via the X site. Such an indirect interaction makes the temperature  $T^*$  where the SHE feels the effects of spin correlations. In AuFe, on the other hand, the Fe impurity has both properties. With such an *on-site* interaction,  $T^* = T_g$  and a clear difference between ZFC and FC can be seen even in the AHE resistivities. Further investigations using different combinations of host and impurity metals are needed to unveil all the details.

In summary, we have studied the SHEs and AHEs in the spin glass systems using the CuMnBi ternary alloys. The SH angle  $|\alpha_H^{\text{3D}}|$  of  $\text{Cu}_{98}\text{Mn}_{1.5}\text{Bi}_{0.5}$  at  $T = 50$  K coincides with that of  $\text{Cu}_{99.5}\text{Bi}_{0.5}$ . With decreasing temperature, however, it starts to decrease at  $T^* = 4T_g$  and becomes 7 times smaller at  $0.5T_g$ . With decreasing concentrations of the Mn impurities,  $T^*$  shifts to lower temperatures. These results suggest that the SHE could be exploited to probe fluctuating spin states in complex spin structures such as spin liquids.

We acknowledge fruitful discussions with K. Kobayashi, M. Ferrier, K. Tanabe, T. Arakawa, Y. Matsumoto, T. Kato, and H. Akai. We thank H. Mori, A. Ueda, J. Yoshida, and H. Idzuchi for their technical support on the magnetization measurements, and Y. Iye and S. Katsumoto for the use of the lithography facilities. This work was supported by Grants-in-Aid for Scientific Research (No. 24740217, No. 23244071, and No. 60245610) and also by Foundation of Advanced Technology Institute.

\*niimi@phys.sci.osaka-u.ac.jp

Present address: Department of Physics, Osaka University, Toyonaka, Osaka 560-0043, Japan.

- [1] K. Binder and A. P. Young, *Rev. Mod. Phys.* **58**, 801 (1986).
- [2] R. Monasson, R. Zecchina, S. Kirkpatrick, B. Selman, and L. Troyansky, *Nature (London)* **400**, 133 (1999).
- [3] S. Nagata, P. H. Keesom, and H. R. Harrison, *Phys. Rev. B* **19**, 1633 (1979).
- [4] J. J. Prejean, M. J. Joliclerc, and P. Monod, *J. Phys. (Paris)* **41**, 427 (1980).
- [5] A. F. J. Morgownik and J. A. Mydosh, *Phys. Rev. B* **24**, 5277 (1981).
- [6] P. G. N. de Vegvar, L. P. Lévy, and T. A. Fulton, *Phys. Rev. Lett.* **66**, 2380 (1991).

- [7] T. Capron, G. Forestier, A. Perrat-Mabilon, C. Peaucelle, T. Meunier, C. Bäuerle, L. P. Lévy, D. Carpentier, and L. Saminadayar, *Phys. Rev. Lett.* **111**, 187203 (2013).
- [8] H. Vloeberghs, J. Vranken, C. Van Haesendonck, and Y. Bruynseraede, *Europhys. Lett.* **12**, 557 (1990).
- [9] D. Petit, L. Fruchter, and I. A. Campbell, *Phys. Rev. Lett.* **88**, 207206 (2002).
- [10] T. Taniguchi, K. Yamanaka, H. Sumioka, T. Yamazaki, Y. Tabata, and S. Kawarazaki, *Phys. Rev. Lett.* **93**, 246605 (2004).
- [11] G. Tataru and H. Kawamura, *J. Phys. Soc. Jpn.* **71**, 2613 (2002).
- [12] Y. Niimi, M. Morota, D. H. Wei, C. Deranlot, M. Basletic, A. Hamzic, A. Fert, and Y. Otani, *Phys. Rev. Lett.* **106**, 126601 (2011).
- [13] Y. Niimi, Y. Kawanishi, D. H. Wei, C. Deranlot, H. X. Yang, M. Chshiev, T. Valet, A. Fert, and Y. Otani, *Phys. Rev. Lett.* **109**, 156602 (2012).
- [14] Y. Niimi, H. Suzuki, Y. Kawanishi, Y. Omori, T. Valet, A. Fert, and Y. Otani, *Phys. Rev. B* **89**, 054401 (2014).
- [15] See Supplemental Material at <http://link.aps.org/supplemental/10.1103/PhysRevLett.115.196602> for sample preparation and for extra data on the SHE in CuMnBi, which includes Refs. [16–19].
- [16] T. Wakamura, N. Hasegawa, K. Ohnishi, Y. Niimi, and Y. C. Otani, *Phys. Rev. Lett.* **112**, 036602 (2014).
- [17] P. Jacquod, R. S. Whitney, J. Meair, and M. Büttiker, *Phys. Rev. B* **86**, 155118 (2012).
- [18] A. Fert, *J. Phys. F* **3**, 2126 (1973).
- [19] A. Fert and P. M. Levy, *Phys. Rev. Lett.* **106**, 157208 (2011).
- [20] A. Fert, A. Friederich, and A. Hamzic, *J. Magn. Magn. Mater.* **24**, 231 (1981).
- [21] A. Fert and P. M. Levy, *Phys. Rev. Lett.* **44**, 1538 (1980).
- [22] P. M. Levy and A. Fert, *Phys. Rev. B* **23**, 4667 (1981).
- [23] H. Bouchiat, N. de Courtenay, P. Monod, M. Ocio, and P. Refregier, *Jpn. J. Appl. Phys.* **26**, 1951 (1987), Suppl 26-3.
- [24] W.-Y. Wu, G. Mozurkewich, and R. Orbach, *Phys. Rev. B* **31**, 4557 (1985).
- [25] H. Mahdjour, C. Pappa, R. Wendler, and K. Baberschke, *Z. Phys. B* **63**, 351 (1986).
- [26] D. L. Leslie-Pelecky, F. VanWijland, C. N. Hoff, J. A. Cowen, A. Gavrin, and C.-L. Chien, *J. Appl. Phys.* **75**, 6489 (1994).
- [27] A. H. El-Sayed, S. Hedewy, and A. El-Samahy, *J. Phys. Condens. Matter* **1**, 10515 (1989).
- [28] S. Takahashi and S. Maekawa, *Sci. Tech. Adv. Mater.* **9**, 014105 (2008).
- [29] Y. J. Uemura, T. Yamazaki, D. R. Harshman, M. Senba, and E. J. Ansaldo, *Phys. Rev. B* **31**, 546 (1985).
- [30] M.-K. Hou, M. B. Salamon, and T. A. L. Ziman, *Phys. Rev. B* **30**, 5239 (1984).
- [31] R. S. Hayano, Y. J. Uemura, J. Imazato, N. Nishida, T. Yamazaki, and R. Kubo, *Phys. Rev. B* **20**, 850 (1979).
- [32]  $\tau_{sk}$  is defined as  $m/(ne^2\rho_{SHE}^{3D})$ , where  $m$  and  $n$  are the mass of the conduction electron and the electron density, respectively.
- [33] D. H. Wei, Y. Niimi, B. Gu, T. Ziman, S. Maekawa, and Y. Otani, *Nat. Commun.* **3**, 1058 (2012).
- [34] C. Du, H. Wang, F. Yang, and P. C. Hammel, *Phys. Rev. B* **90**, 140407(R) (2014).